Int. J. Nanoelectronics and Materials **7** (2014) 9-16

Thermal and photoluminescence properties of Nd^{3+} doped tellurite nanoglass

N. A. M. Jan*, M. R. Sahar

Advanced Optical Material Research Group, Department of Physics, Faculty of Science, Universiti Teknologi Malaysia, 81310, Skudai, Johor Bahru, Johor, Malaysia.

Abstract

Series of glass based on $(75\text{-}x)TeO_2\text{-}15MgO\text{-}10Na_2O\text{-}xNd_2O_3$, where x=0, 1.0, 2.0, and 3.0 are synthesized by conventional melt-quenching technique. The nanoglass particles are derived from heat treatment of this glass near crystallisation temperature for 3 hours. The existence of nanocrystalline nature of this glass is confirmed by x-ray diffraction (XRD) technique followed by calculation using Scherrer equation. Meanwhile, the crystallization temperature, Tc determined using Differential thermal analysis (DTA). The fluorescence spectra of Nd^{3+} ions exhibit emission transition of $^2P_{3/2}\rightarrow{}^4I_{9/2}$, $^4G_{7/2}\rightarrow{}^4I_{9/2}$, $^2H_{11/2}\rightarrow{}^4I_{9/2}$, and $^4F_{9/2}\rightarrow{}^4I_{9/2}$ under 765 nm excitation wavelengths.

Keywords: Tellurite glass, thermal, photoluminescence, nanoglass.

1. Introduction

Tellurite glass is of technical and scientific interests on the account of their easy fabrication at low temperature, high refractive index, and extended infrared transmission. It has been considered as a promising material for its widespread use in optical fiber technology [1]. Since the strong rare-earth ions-host interaction results in efficient upconversion emissions, tellurium has been recognized as a suitable glass host for the laser application [2]. In addition, most tellurite glasses have a great rare-earth ion solubility and low phonon energy which enables to design efficient laser and amplifier devices [3]. Therefore, the combination of rare earth with tellurite glasses has been a key to the development of many areas like optical sensing, biochemical studies and biomedical [4, 5].

Previously, there are many studies succeeded in spectroscopic characterization of tellurite glass doped with neodymium. Neodymium doped all-solid-state laser sources have been identified as the most efficient laser sources for numerous applications in the fields of high-resolution spectroscopy. The development of low threshold high gain host media for Nd^{3+} ion doping was encouraged by the applications in these areas. It is obvious that the enlargement of host material for Nd^{3+} ions requires optimum material properties. They are characterized by a low content of OH^- groups and a low frequency phonon spectrum. It is because these properties make it possible to reduce excitation losses due to multiphonon relaxation. Addition, the OH^- free tellurite glasses which are used as host material for Nd^{3+}-doped laser glasses have been a subject of increasing interest for optoelectronic applications. It is because of their high refractive index and low phonon energies [6].

*) For correspondence, E-mail: amaninamatjan@yahoo.com

In this work, we report to prepare the tellurite glass doped with neodymium via melt quenching technique and derived nanoglass will confirmed by x-ray diffraction followed by Scherrer equation. In addition, the effect of dopant throughout all samples towards the optical properties in terms of luminescence will be investigated.

2. Experiment

Nd^{3+} doped magnesium-tellurite glasses of compositions (75-x)TeO_2-15MgO-10Na_2O-xNd_2O_3, where x=0, 1.0, 2.0, and 3.0. The system was prepared by melt quenching technique. They were heated in furnace and melted in the range of 850℃-900℃ depending on the glass composition. The glass samples were annealed for about 2 hours at 300℃ to remove thermal stress before being cooled down to room temperature. Thermal properties of the glass is analyzed using DTA, Perkin Elmer DTA-7 Series System. The glass is then heat treated near Tc for 3 hours. The existence of nanoglass has been calculated using the Scherrer equation [1] given by:

$$D = \frac{0.9\lambda}{\beta \cos\theta} \tag{1}$$

where λ is the wavelength of X-ray radiation (CuKa 1.5406x10^{-10}) and β is the FWHM of the peak at 2θ. The luminescence spectra is obtained by using Nanosecond Luminescence Spectroscopy System, Ekspla Model NT340/1 excited at 765nm using tunable Nd: YAG laser system. Each sample is scanned for radiation spectral wavenumber in the range of 200 – 900 cm^{-1} at room temperature.

3. Results and Discussion

Table 1 shows a series of TeO_2 - Na_2O-MgO glass system doped with Nd^{3+} that have been prepared by melt-quenching technique as shown in Table 1.

Table 1: Series of (75-x)TeO_2-15MgO-10Na_2O-xNd_2O_3 (x=0, 1.0, 2.0, and 3.0) glass system

No. of Sample	TeO_2 (mol%)	MgO (mol%)	Na_2O (mol%)	Nd_2O_3 (mol%)
S1	75	15	10	0
S2	74	15	10	1
S3	73	15	10	2
S4	72	15	10	3

The glass is visually transparent, appearing light brownish yellow due to Nd^{3+} doping. The glass samples are heat treated at Tc-50℃ for 3 hours.

3.1 Differential Thermal Analysis

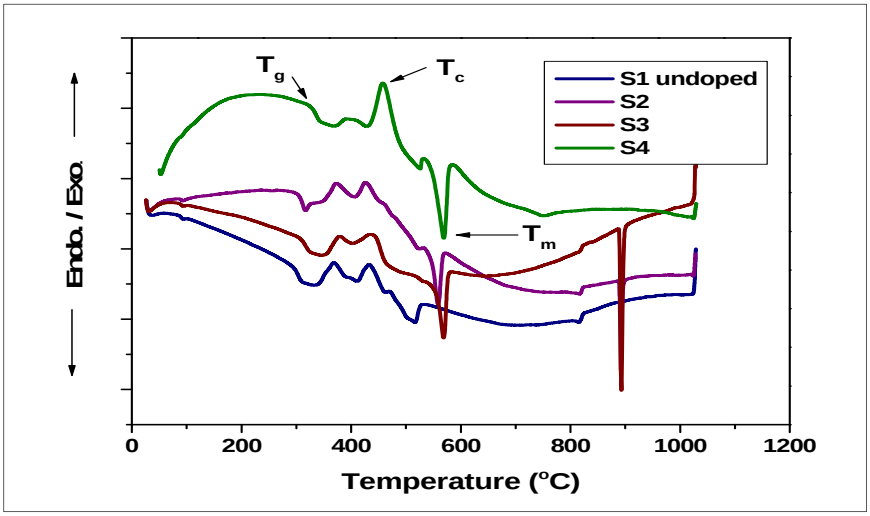

Fig.1: The thermal characteristic of the glass as measured by differential thermal analysis (DTA).

The thermal characteristics are theb summarized in Table 2. The glass transition temperature T_g, crystallisation temperature T_c, and melting temperature T_m from a single DTA scan were calculated and compared in tables 2.The glass T_g, T_c, and T_m temperatures all have increased with increasing Nd_2O_3 concentration in the glass system.

Table 2: DTA results of (75-x)TeO_2-15MgO-10Na_2O-xNd_2O_3 (x=0, 1.0, 2.0, and 3.0) tellurite glasses

No. of Sample	**T_g**	**T_c**	**T_m**	**Stability $S=T_c-T_g$**	**Tendency $k_g = \frac{T_c-T_g}{T_m-T_c}$**
S1	300.43	368.42	516.00	67.99	0.46
S2	303.41	373.27	891.94	69.86	0.13
S3	307.87	378.92	892.97	71.05	0.14
S4	323.32	391.49	568.98	68.17	0.38

Thermal stability of glasses is one of the most important properties for glasses perform fabrication and is a measure of degree of disorder of glassy state. There are two widely used parameters for evaluating thermal stability of glasses from characteristic temperatures. These equations are defined as follows [8]:

$$S = T_c - T_g \tag{2}$$

$$k_g = \frac{T_c - T_g}{T_m - T_c} \tag{3}$$

The glass thermal stability is assessed by employing S and k_g parameters. The S value is an implication of the devitrification tendency of glass when heated above T_g. It defines the temperature range for glass drawing. The larger S and the smaller difference between crystallization temperature, T_c and melting temperature T_m slow down crystallization process and facilitate glass formation.

3.2 X-Ray Diffraction

Figure 2 shows the x-ray diffraction spectra of sample 1 after heat treatment. It can clearly be seen that the glass is still dominated by the amorphous structure as shown in Fig. 1. However, if the crystalline size is calculated using the Scherrer equation at the Nd^{3+} peaks, the result can be obtained. The XRD pattern of this sample is identical to the previous sample, showing peak at 26.5° is superimposed; these peak can be attributed to TeO^2 crystalline phases [9]. From the FWHM of the intense diffraction peak of transparent tellurite nanoglass, the average crystallite size (diameter, d) is in range 2-14 nm.

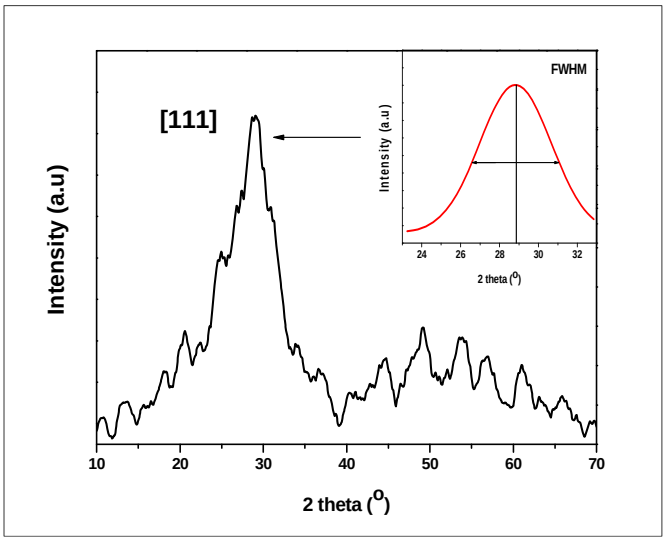

Fig. 2: XRD pattern of the glass system after heat-treated.

3.2 Photoluminescene Spectra

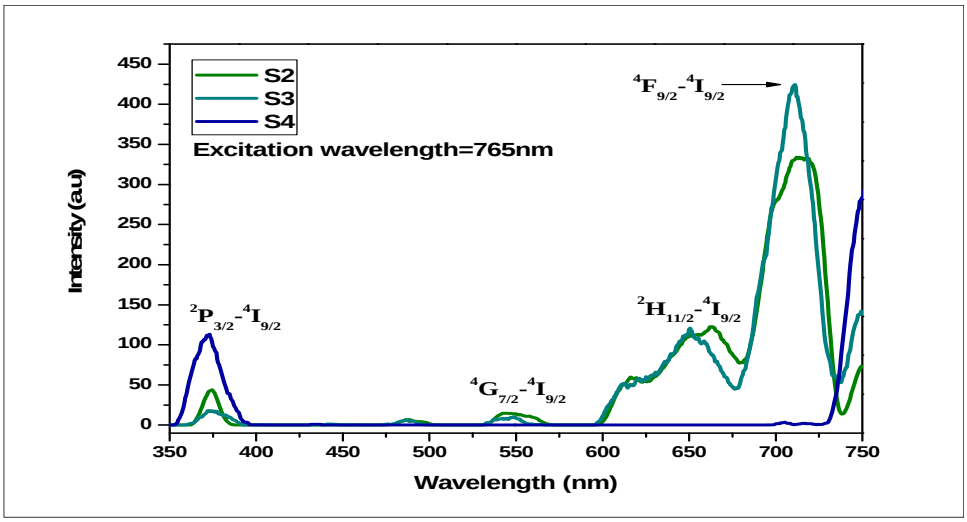

Fig. 3: Emission spectrum from the heat-treated neodymium-doped Na_2O-MgO-TeO_2 nanoglass with different concentration of neodymium.

Fig. 3 shows visible up-conversion emission characteristic spectrum of radiation emanating from a neodymium-doped tellurite nanoglass with excitation at the wavelength of 765nm. It can be seen from Fig. 3 that apart from a green emission transition at 547 nm corresponding to the $^4G_{7/2}\rightarrow{}^4I_{9/2}$ transition of the neodymium ions, a relatively weak ultraviolet emission transition at 373 nm ($^2P_{3/2}\rightarrow{}^4I_{9/2}$) and red emission transition at 656 nm and 713 nm ($^2H_{11/2}\rightarrow{}^4I_{9/2}$ and $^4F_{9/2}\rightarrow{}^4I_{9/2}$) respectively are also observed. The up-conversion luminescence transition spectrum of $^4D_{3/2}\rightarrow{}^4I_{J+1}$ or $^2P_{3/2}\rightarrow{}^4I_J$ (J=13/2,11/2,9/2) was found to be essentially similar as those reported in Refs.10 and 11 and energy transfer $^4G_{7/2}$ has been previously reported [12]. An ultraviolet emission at about 345 nm has not been observed [13].

Based on Fig. 3, it can also be seen that the red emission intensity increases with Nd concentration. The intensity not make any different at green band and $^2H_{11/2}\rightarrow{}^4I_{9/2}$ transition of emission band but there is slightly shift of the peaks position, which indicates the interaction of ions between Nd^{3+} sites. It can be observed that the intensity of $^2P_{3/2}\rightarrow{}^4I_{9/2}$ transition increases due to the increasing concentration of Nd but peaks of S4 can be seen disappeared at transition in range 450 nm-725 nm. It is because at the high Nd concentration, the luminescence will be quenched by energy transfer processes due to interactions between Nd ions and OH^- groups.

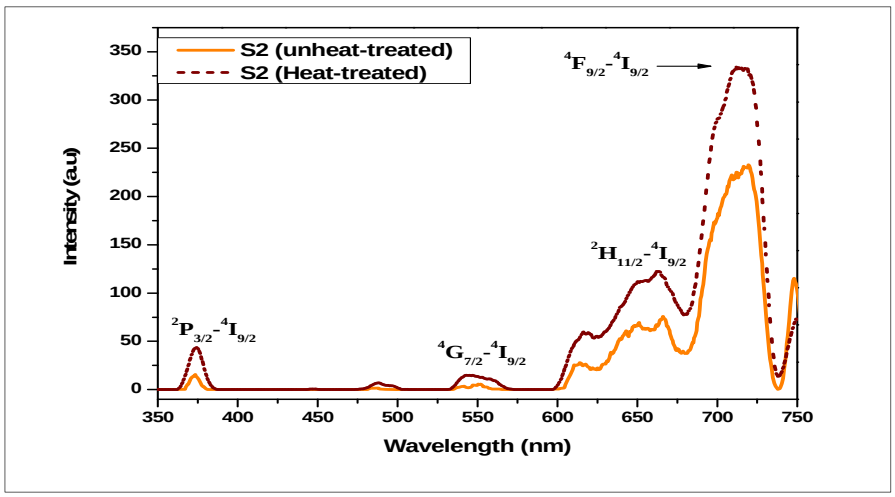

Fig. 4: Comparison of the emission spectra from Na_2O-MgO-TeO_2 glass containing 1 mol% Nd_2O_3 with heat-treated and unheat-treated glass under an excitation of 765 nm.

Emission spectra of 1 mol% Nd in heat-treated and unheat-treated glass system is shown in Fig. 4 using 765 nm excitation wavelengths. The emission peaks apparent at 373 nm, 547 nm, 656 nm, and 713 nm (same as Fig.3). The 765 nm excitation is dominated by the emission near 713 nm which is the transition is from the thermally populated $^4F_{7/2}$ state to $^4I_{9/2}$ [14]. The intensity of heat-treated sample shows enhancement after heat treatment.

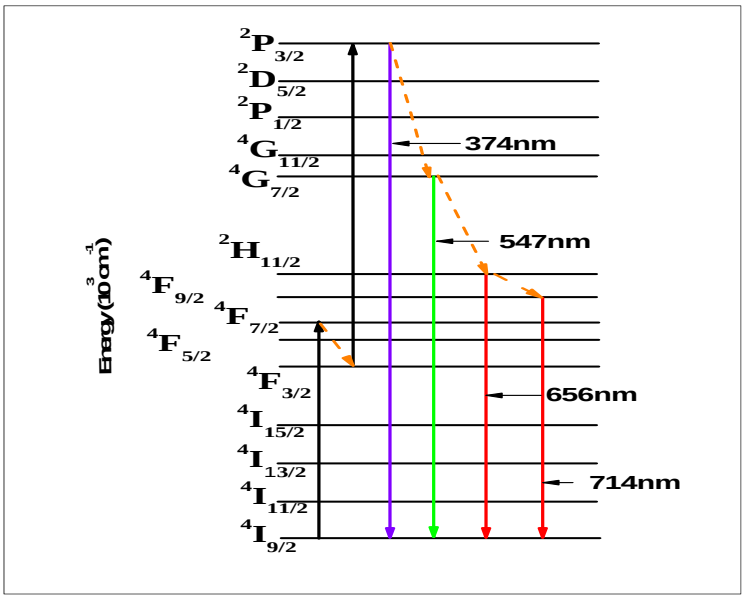

Fig. 5: Energy-level scheme describing the up-conversion emission from the neodymium-doped Na_2O-MgO-TeO_2 nanoglass upon an excitation at 765nm.

Fig. 5 is a schematic diagram describing the mechanism of the up-conversion emission from a neodymium ion via a two-photon absorption process. In this process, Nd^{3+} ions are pumped with 765 nm excitation wavelength through the ground state absorption (GSA) they excite to the $^4F_{7/2}$ level. Using excited state absorption (ESA) mechanism [14], the electron rapidly decays nonradiatively to the metastable $^4F_{3/2}$ state. Ref. 15 reported that this metastable state has a quite long lifetime and thus the electron has a high chance to absorb a second 765 nm photon before the electron further decays downwards. Then, it gets

excited to the $^2P_{3/2}$ state. Afterwards, some electrons will decay radiatively to the $^4I_{9/2}$ state as shown in the energy diagram of Fig. 5. As they populated the $^2P_{3/2}$ level, some of the Nd^{3+} ions relaxed radiatively to $^4I_{9/2}$ level thus emitting the enission spectra centered at 374 nm. Some of the Nd^{3+} ions are found relax non-radiatively to lower level $^4G_{7/2}$, $^2H_{11/2.}$and $^4F_{9/2.}$ The Nd^{3+} ions at $^4G_{7/2}$ are then decay to $^4I_{9/2}$ by emitting the emission spectra centered at 547 nm in green region. Whereby, the Nd^{3+} ions that emitting the red emission spectra are centered at 656 and 714 nm as the decay to $^2H_{11/2.}$and $^4F_{9/2}$ level respectively [16].

4. Conclusion

Some conclusions can be made and summarize as follows: the system of neodymium-doped Na_2O-MgO-TeO_2 nanoglass with different Nd_2O_3 concentration has successfully been made by melt-quenching technique. Differential thermal analysis (DTA) has been employed to verify the glass transition (T_g), crystallization (T_x) and melting temperatures (T_m). The nanostructured of the glass has been determined by calculating the crystalline size in range 2-11 nm of the glass using the Scherrer method. The analysis detail on the visible emission process from the glass system to verify its luminescence performance has been carried out. The results showed the emission of four visible luminescence bands centered on 374, 547, 656, and 714 nm as to correspond to the $^2P_{3/2}\rightarrow{}^4I_{9/2}$, $^4G_{7/2}\rightarrow{}^4I_{9/2}$, $^2H_{11/2}\rightarrow{}^4I_{9/2}$, and $^4F_{9/2}\rightarrow{}^4I_{9/2}$ transitions of the Nd^{3+} ions respectively.

Acknowledgments

The authors gratefully acknowledge the financial support from Ministry of Higher Education through grant Vot. 4F083 and Universiti Teknologi Malaysia under Vot. 02J77 (GUP/MOHE).

References

[1] J. S. Wang, E. M. Vogel, E. Snitzer, Opt. Mat Vol. **3** (1994) 187
[2] Koepke, Cz., Wisniewski, K., Sikorski, L., Piatkowski, D., Kowalska, K., Naftaly, M., J. Optical Materials **28** (2006) 129
[3] S. Shen, A. Jha, *Trans Tech Publ*. (2008)
[4] Kumar, K., Rai, S. B, Anita Rai, J. Spectrochimica Acta Part A **71** (2008) 508
[5] Wade, S. A., Collins, S. F., Baxter, G. W., J. Appl. Physis **94** (2003) 474
[6] R. Rajeswari, S. S. Babu, C. K. Jayasankar, J. Spectrochimica Acta Part A **77** (2010) 135
[7] A. Tarafder, A. R. Molla, B. Karmakar, J. Am. Ceram. Soc., **93(10)** (2010) 3244
[8] W. G. Jordan, A. Jha, J. Thermal Analysis Vol. **42** (1994) 759
[9] Arshpreet Kaur, Atul Khanna, Carmen Pesquera, Fernando González, Vasant Sathe, Journal of Non-Crystalline Solids **356** (2010) 864Journal of Non-Crystalline Solids 356 864–872
[10] K. Annapurna, R. N. Dwivedi, P. Kundu, S. Buddhudu, Mater. Lett. **57** (2003) 2095
[11] B. Zhou, Y. Zhou, Y. L. Lam, C. Y. Chan, C. H. Kam, S. D. Cheng, and S.Buddhudu, Opt. Commun. **182** (2000) 151

[12] F. Ramos-Lara, D. Jaque, J. Garcia-Sole, G. U. Caldino, J. Phys. Condens. Matter. **12** (2000) L441
[13] W. Que, Z. Sun, X. Hu, J. Appl. Physis. **98** (2005) 093518
[14] A. T. Stanley, E. A. Harris, T. M. Searle, J. M. Parker, J. Non-Crys. Solids **161** (1993) 235
[15] J. C. Wright, Top. Appl. Phys. **15** (1976) 239
[16] Azman, K., Sahar, M. R., Rohani, M. S., World Academy of Science, Engineering and Technology **64** (2010)